Rev.Adv.Mater.Sci. 15(2007) 167-172

COLOR DEPENDENCY ON OPTICAL AND ELECTRONIC PROPERTIES OF TiN_x THIN FILMS

N. Kalfagiannis and S. Logothetidis

Aristotle University of Thessaloniki, Physics Department, Laboratory for Thin Films – Nanosystems & Nanometrology (LTFN), GR-54124 Thessaloniki, Greece

Received: January 22, 2007

Abstract. In-situ and real-time Spectroscopic Ellipsometry (SE) has been employed for the investigation of the correlation between visual appearance and optical and electronic properties of TiN_x nanocrystalline coatings. These films were deposited onto c-Si substrates by Reactive Magnetron Sputtering in an unbalanced configuration. It has been found that the N_2 content in the gas discharge, which controls the nitrogen composition in the film, plays a major role in the color control for TiN_x films. The effect of the nitrogen amount on the color of the TiN_x thin films has been investigated by the analysis of the measured pseudo-dielectric function $\langle\varepsilon(\omega)\rangle$. We also present a comparison between the electronic properties of these films and TiN_x coatings fabricated with Balanced Magnetron Sputtering in similar deposition conditions. Insights on the optical and electronic properties were arisen from the analysis of SE spectra, using the combined Drude-Lorentz model, which describes the optical response of the conduction and valence electrons. The energy, strength and broadening of the interband transitions as well as intraband absorption provided by the conduction electron density were studied with respect to the applied bias voltage, V_b.

1. INTRODUCTION

Titanium nitride (TiN_x) thin films exhibit a unique combination of high hardness, good chemical inertness, beautiful lustrous color, and excellent wear resistance and thus are widely used as wear-resistant coatings for tools and wear parts, as well as surface decoration for commercial goods [1-3]. Decorative coatings are designed not only for attractive surface coloration, but also to protect the substrate material against wear and corrosion [4,5]. In this respect, TiN_x thin films have attracted the interest for decorative applications. Spectroscopic Ellipsometry (SE) can provide major information on their optical and electronic properties and has been applied successfully to characterize the color of various decorative coatings [6-8].

In this work, we investigate the influence of N_2 partial pressure and the applied negative bias voltage (V_b) at the substrate on the TiN_x optical properties in order to obtain precise color control using SE, which addresses the optical properties of thin sputtered TiN_x films in terms of their complex dielectric function ($\varepsilon(\omega) = \varepsilon_1 + i\varepsilon_2$). For the consideration of the visual effect of the coatings we used the Tauc-plot method, in order to calculate the onset of the interband transitions and thus the fundamental gap (E_g) which is responsible for the color presence. This method provides a relatively wide band gap via linear extrapolation of $[E\times\varepsilon_2(\text{Å})]^{1/2}$ to zero ordinate [9].

Furthermore, we analyzed the dielectric function of TiN_x films based on the intraband and interband transitions. The intraband absorption was studied in terms of the free electron (Drude) model [10,11] and the interband transitions with the Lorentz oscillator model [10].

Corresponding author: S. Logothetidis, e-mail: logot@auth.gr

© 2007 Advanced Study Center Co. Ltd.

2. EXPERIMENTAL

TiN_x thin films were deposited on n-type c-Si(100) by dc reactive unbalanced magnetron sputtering from a Ti target of 99.95% purity in a high vacuum chamber (base pressure ~$1.3 \cdot 10^{-4}$ Pa), using working (Ar) and reactive (N_2) gas (99.999% purity) at partial pressures of 0.347 Pa and 0.307 – 0.427 Pa, respectively. Prior to the loading into the deposition chamber the c-Si wafers were cleaned in air using chemical etching in an ultrasonic bath, following a standard chemical procedure [12], and in vacuum with dry low energy Ar ion etching in order to remove the native SiO_2. The deposition has been performed at target power 2.5 kW for various values of bias voltage, V_b, applied to the substrate, from 0 (referred also as floating condition, V_f = +20 V) to -150 V during deposition and N_2 partial pressure (0.307 – 0.427 Pa). The deposition time was adjusted based on previous deposition rate data [13] in order to deposit films with maximum thickness ~100 nm.

In situ and real-time SE spectra were obtained with a Jobin–Yvon Horiba MultiWavelength Spectroscopic Ellipsometer of 16 wavelengths, operating in the energy region 1.5 – 4.22 eV. The MWE monitoring results concerning the variations of the unscreened plasma energy with time can be used to identify the stoichiometry (x) of the TiN_x films, based on the results reported in the literature [14]. The speed of the real-time measurements depends on the integration time (IT) used for the acquisition at each wavelength. The smaller IT value, the closest monitor of the growth processes is achieved, since the acquisition time for every step measurement sampling time ST, which embodied the 16 wavelengths, is defined by IT. The smaller IT 10 ms were set by the accuracy and the reproducibility of the MWE measurements and the deposition rate of the material. In addition to MWE measurements, ex-situ SE measurements, in the energy region 1.5-6.5 eV, were performed in order to obtain more detailed information about the energy position, the strength and the broadening of the interband transitions of the films and be compared with the properties of TiN_x films deposited in a balanced magnetic field. This is due to the more extended spectral range of the ex-situ measurement and also the use of a monochromator which gives more accurate spectra measurement.

3. RESULTS AND DISCUSSION

SE is a nondestructive, surface-sensitive technique which determines the ratio between the parallel and

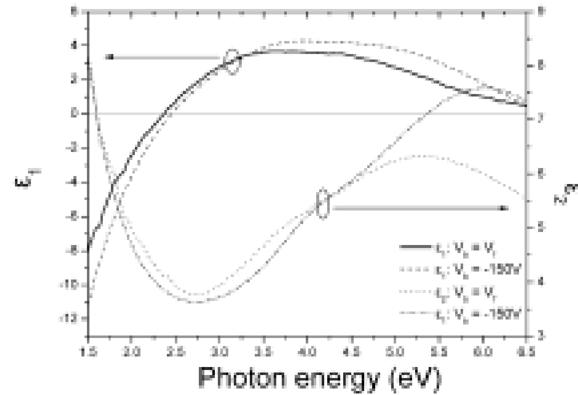

Fig. 1. Real (ε_1) and imaginary (ε_2) parts of the dielectric function of two representative TiN_x thin films grown for V_f and V_b = -150 Volts.

perpendicular complex reflection coefficients, through which the complex dielectric function, $\varepsilon(\omega)=\varepsilon_1(\omega)+i\times\varepsilon_2(\omega)$ is calculated [15]. The determination of the complex dielectric function enables the investigation of the material electronic structure ($\varepsilon_2(\omega)$ is directly related to the conduction electron density and the density of states for interband absorption and structural characteristics). Since the dielectric function is the consequence of the electronic properties, it provides direct information about the origin of the spectral reflectivity and absorption. Therefore, it allows the investigation of the effect of changes in composition and (electronic) structure on the optical properties and hence the color of the material [4].

In the case of a thin film, the measured $\varepsilon(\omega)$ by SE accounts for the effect of the substrate and film thickness in addition to the film optical properties. However, for TiN_x films thicker than 60 nm, SE directly provides the complex dielectric function of the bulk film, without any contribution from the Si substrate [16]. Fig. 1 shows the real (ε_1) and the imaginary (ε_2) parts of $\varepsilon(\omega)$ obtained from two representative TiN_x films deposited at RT at V_b = V_f and V_b = -150 V.

Of special interest is the unscreened plasma energy ω_{pu} of the material [17]. In an ideal metal with all electrons free, ω_{pu} is defined by the energy position where the real part of the dielectric function is almost zero (ε_1 = 0). However, in real metals, the existence of interband transitions (bounded electrons) at energies lower than ω_{pu} shifts the point where ε_1 = 0 to lower energy, which is called

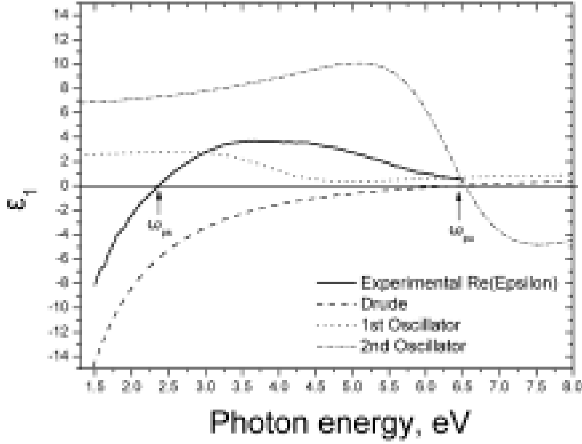

Fig. 2. The experimental real part (ε_1) of dielectric function of TiN_x thin film grown for V_f. Individual contributions of the Drude term (dashed line) and the two Lorentz oscillators (dot, dashed-dot lines) are presented separately.

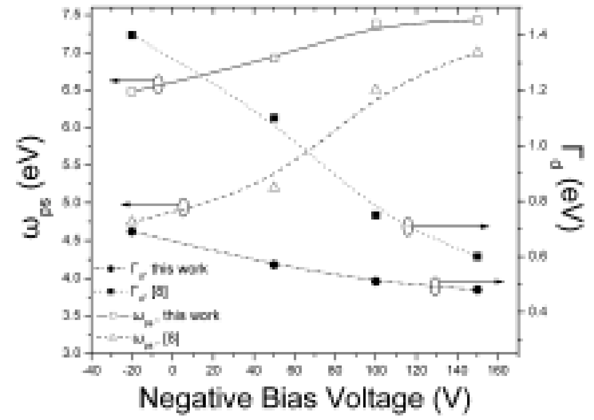

Fig. 3. Variation of the Drude parameters in respect to the bias voltage – a comparison between the calculated values and values that have been reported in literature [9].

screened plasma energy ω_{ps}. The ω_{ps} is shown in Fig. 2, denoted by arrows in the ε_1 spectra of a TiN_x thin film grown at $V_b = V_f$. The individual contributions of the Drude term (dashed line) describing the optical response of the Ti 3d conduction electrons, and the two Lorentz oscillators located at 3.65 eV (dot line) and 6.15 eV (dashed-dot line), which correspond to the TiN_x interband transitions, are presented separately.

The unscreened plasma energy, ω_{pu}, depends on the concentration of the conduction electrons in the film and is defined by the relation [10]:

$$\omega_{pu} = \sqrt{\frac{Ne^2}{\varepsilon_0 m^*}}, \quad (1)$$

where N is the conduction electron density, e is the electron charge, ε_o is the permittivity of free space, and m^* is the electron effective mass, in SI units. Since ω_{pu} is directly correlated with the conduction electron density, it can be used to determine the metallic character of the TiN_x. The dielectric functions of TiN_x films were analyzed, through appropriate modeling, with regards to the contributions of intraband and interband transitions described by the Drude term and two Lorentz oscillators, respectively [10]:

$$\varepsilon = \varepsilon_\infty - \frac{\omega_{pu}^2}{\omega^2 - i\Gamma_d\omega} + \sum_{j=1}^{2} \frac{f_j\omega_{0j}^2}{\omega_{0j}^2 - \omega^2 + i\gamma_j\omega}. \quad (2)$$

In Eq. (2), ε_∞ is a background constant, larger than unity, due to the contribution of the higher energy transitions that are not taken into account in the Lorentz term. The Drude term is characterized by the unscreened plasma energy ω_{pu} and the damping factor Γ_d. This parameter is due to the scattering of electrons and, according to the free-electron theory, is the inverse of the electron relaxation time τ_d. Each of the Lorentz oscillators is located at an energy position ω_{0j}, with strength f_j and damping (broadening) factor γ_j.

The values of the unscreened plasma energy (ω_{pu}) appear to be slightly higher comparing to the values reported in literature [15] as it is shown in Fig. 3. This is due to the more intensive ion bombardment of the surface of the growing film, which introduces the unbalanced magnetron sputtering technique. Increasing the energy, which is transported in the substrate, results to higher nucleation density eliminating Ti-vacancies and finally leading to a more dense structure [18]. The higher the

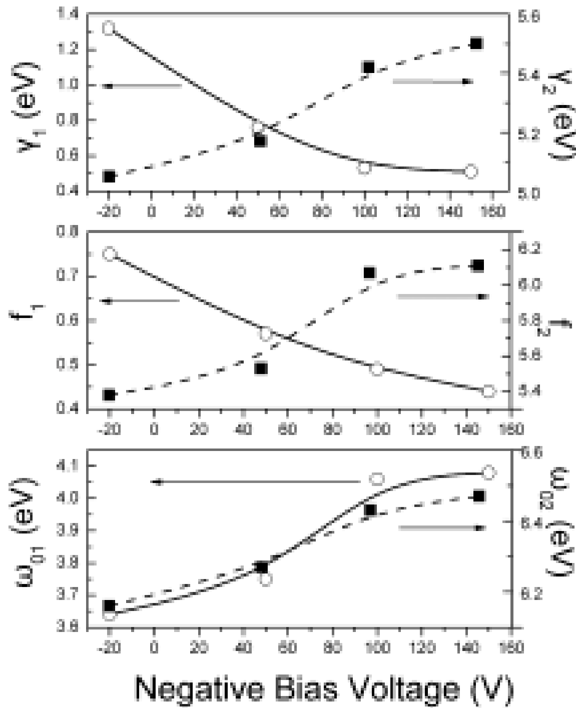

Fig. 4. The variation of the Lorentz oscillator parameters (ω_{0j}, γ_j, $\mathbf{f}_j$) in respect to the bias voltage.

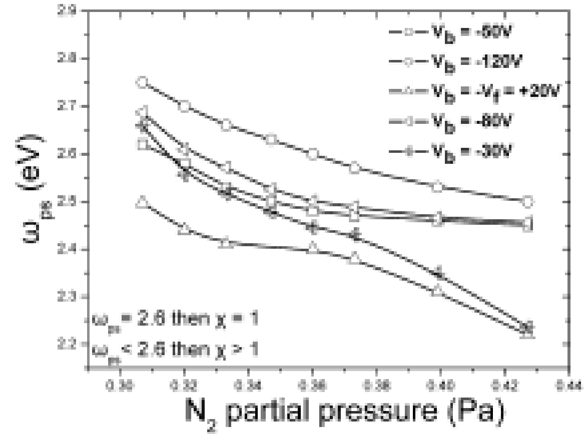

Fig. 5. The variation of ω_{ps} versus N_2 partial pressure. As N_2 partial pressure increases in the gas discharge the [N]/[Ti] ration increases also leading to lower values of ω_{ps}.

values of mass density, the higher the number of free electrons of the film, leading to higher values of ω_{pu}. The broadening factor of the Drude term, Γ_d, in bulk materials depends mainly on the defects (Ti vacancies), and therefore mass density determines the Mean Free Path (MFP). On the other hand, in nanocrystalline coatings the MFP of free electrons is comparable to the grain size. Thus, increasing the ion bombardment either by increasing the V_b or the plasma density leads to lower values for Γ_d.

The parameters of the Lorentz oscillators in TiN_x thin films vary with the deposition conditions such as V_b as shown in Fig. 4. The negative V_b, applied to the substrate, induces the ion bombardment of the film surface during deposition, changing its structure and stoichiometry. Values of ω_{01}, ω_{02} are higher as the unbalanced magnetic field further induces the ion bombardment. This fact affects also the values of f_1 and f_2 as well. More specifically, it leads to lower values for f_1 and higher values for f_2. This is due to the defacement of energy bands near the centre of the Brillouin zone, in the case of the first oscillator, and the activation of transition across the high symmetry lines of the Brillouin zone in the case of the second oscillator, leading to higher values of the f_2 parameter.

The dependence of the γ_1, γ_2 parameters is more complex as they depend not only on the shape and the size of the grains, but also on defects, crystallographic orientation, *etc.* [19].

The visual appearance of a thin film is the consequence of selective absorption / reflection in the visible spectral range. Visible light interacts with the electrons in a metallic material via intraband transitions (interaction with free electrons, described by the Drude model) and interband transitions (interaction with bound electrons, Lorentz model) [20]. For the investigation of the influence of the N_2 partial pressure on the TiN_x physical properties, to obtain precise color control several thin films were fabricated for different values of N_2 partial pressure and bias voltage.

As shown in Eq. (1), the plasma energy is proportional to the square root of N and the density of the free electrons is mainly due to Ti content in the material; the decrease of free electrons with increasing nitrogen content in the TiN_x film will result in a decrease in the plasma energy [14]. Therefore, when the molar x increases, the ω_p decreases and the color of the sample changes from grey to yellow or gold-like (x=1) and then to brown for overstoichiometric material. In order to determine

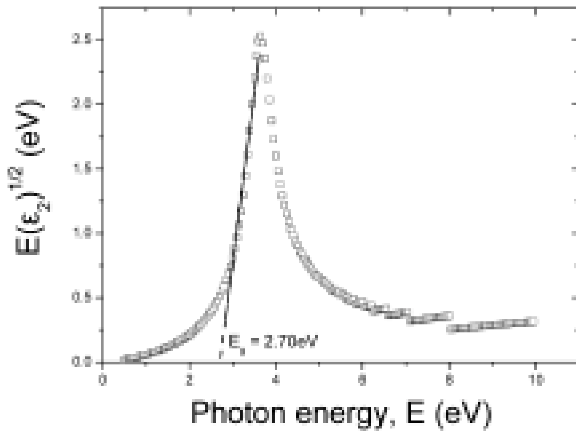

Fig. 6. Tauc-plot method. The extrapolation of the $E\times[\varepsilon_2(E)]^{1/2}$ of the first interband transition in zero coordinate provides the fundamental gap (E_g). This interband transition is responsible for the visual appearance of the films.

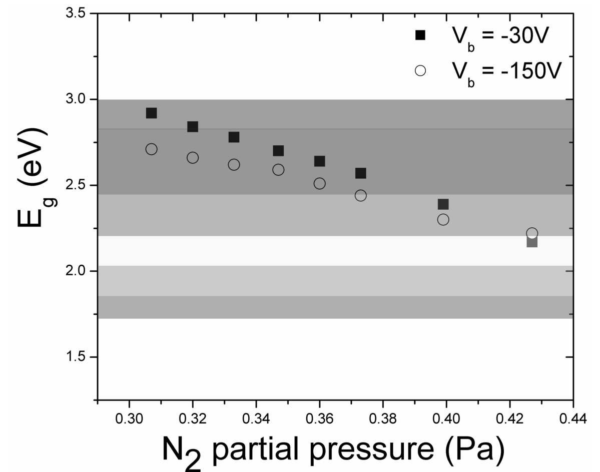

Fig. 7. The calculated values of the fundamental gap (E_g). In the graph it is shown the visual spectra. The color of the films is the complementary of the color that corresponds to each value for the E_g.

the TiN_x films stoichiometry during deposition, we used the value of plasma energy ω_{ps} that was found to be about 2.6 eV when $x = 1$ [21]. Fig. 5 presents the overall results for ω_{ps}, for all the growing films in the different deposition conditions.

The onset of the interband transition is responsible for the color of the TiN_x nanocoatings and occurs at lower energies than the calculated transition energies. This weak absorption, which is the fundamental interband transition, cannot be experimentally identified and discriminated from the strong, dominating contribution of the intraband absorption of the SE spectra at low photon energies. For the determination of this weak interband transition we used the Tauc-Plot method. E_g was determined by the extrapolation of the linear region of the $E\times[e_2(E)]^{-1/2}$ graphic to zero ordinate, as shown in Fig. 6 [9].

This energy gap permits the absorption of a specific wavelength and thus a specific color, as long as E_g is in the visible spectra region. For example, E_g = 2 eV permits the absorption of violet and some blue, but none of the other colors, leading to a yellow color. A yet smaller E_g, lower than 1.71 eV (700 nm), upper limit of the visible spectra, leads to black color, as all light is absorbed. For E_g higher than 3 eV no light in the visible region can be absorbed and so these materials appear to be colorless.

Finally, in Fig. 7 the results for the calculated energy gaps through the Tauc-Plot method are shown for the films grown at V_b = -30 V and -150 V, at various values of N_2 partial pressure. There is also presented the visible color spectra (energy region between 1.71 – 3 eV). The color of the film is the complementary of the color shown in Fig. 7. So, films with E_g between 3 – 2.83 eV appear to be green-yellow, films with E_g between 2.83 – 2.44 eV appear to be yellow and finally films with E_g between 2.44 – 2.11 eV appear to be red.

4. CONCLUSIONS

TiN_x thin films were fabricated using reactive magnetron sputtering in an unbalanced configuration. The coatings were deposited at various values of V_b and N_2 partial pressure. The aim of this work was to investigate the optical response of these films with respect to the V_b and the N_2 partial pressure, and compare the results with TiN_x films developed in same deposition conditions in balanced magnetron sputtering. TiN_x, as metallic material, can be described by the Drude model combined with two Lorentz oscillators that describe the interband transitions. It has been shown that the Drude parameters that describe the behavior of the free electrons follow a specific dependence on the bias voltage. This is due to changes of the stoichi-

ometry and the raise of the mass density of the films leading to raised electron density. On the other hand, Γ_d is decreased as the percentage of defects; thus the mean free path of the free electrons is increased. Moreover, the Lorentz parameters are also influenced by the V_b and it has been confirmed that this dependency is following previous results that associate the energy position and the strength of the oscillators with the size of the unit cell while appointing the broadening as a more complex parameter which depends from the shape of the unit cell, the grain size, structural defects and crystallographic orientation.

In addition to the above analysis we managed to investigate, in-situ, the color of the sputtered TiN_x films through the use of SE. Using the Tauc-Plot method, the onset of the interband transitions has been determined and therefore the prediction of the color of the TiN_x thin films has been realized. We have also correlated these color variations with the N_2 partial pressure, which guides the nitrogen concentration in the films, and therefore with the ω_{ps} and consequently with the stoichiometry (x). Rising the N_2 partial pressure leads to a decrease of ω_{ps} and higher values of [N]/[Ti] ratio and more reddish colors. In the search for new colors in the decorative coatings, SE has been proved to be a power tool for the in-situ control of the color of the films.

ACKNOWLEDGEMENTS

This work has been supported by the Greek General Secretariat for Research and Technology under the PENED03 ED613 Project.

REFERENCES

[1] S. Kadlec, J. Musil and J. Vyskocil // *Surf. Coat. Technol* **54/55** (1992) 249.

[2] M. Y. Al-Jaroudi, H. T. G. Hentzell, S. E. Hornstrom and A. Bengston // *Thin Solid Films* **190** (1990) 2656.

[3] T. Arai, H. Fujita and M. Watanabe // *Thin Solid Films* **154** (1987) 287.

[4] O. Banakh, M. Balzer, M. Fenker and A. Blatter // *Thin Solid Films* **455-456** (2004) 650.

[5] Georg Reiner, Harald Hantsche, Hermann A. Jehn, Uwe Kopacz and Andreas Rack // *Surf. Coat. Technol.* **54-55** (1992) 387.

[6] U. Beck, G. Reiners, I. Urban and K. Witt // *Thin Solid Films* **220** (1992) 234.

[7] Ph. Roquiny, F. Bodart and G. Terwange // *Surf. Coat. Technol.* **116-119** (1999) 278.

[8] U. Beck, G. Reiners, I. Urban and K. Witt // *Thin Solid Films* **220** (1992) 234.

[9] S. Ferlauto, G. M. Ferreira, J. M. Pearce, C. R. Wronski, R. W. Collins, Xunming Deng and Gautam Ganguly // *J. Appl. Phys.* **92** (2002) 2424.

[10] F. Wooten, *Optical Properties of Solids* (Academic, New York, 1972).

[11] N. W. Ashcroft and N. D. Mermin, *Solid State Physics* (Saunders College, Orlando, 1976).

[12] P. Patsalas and S. Logothetidis // *J. Appl. Phys.* **93** (2003) 989.

[13] V.G. Kechagias, M. Gioti, S. Logothetidis, R. Benferhat and D. Teer // *Thin Solid Films* **364** (2000) 213.

[14] S. Logothetidis, I. Alexandrou and A. Papadopoulos // *J. Appl. Phys.* **77** (1995) 3.

[15] P. Patsalas and S. Logothetidis // *J. Appl. Phys.* **90** (2001) 4725.

[16] P. Patsalas and S. Logothetidis // *Surf. Coat. Technol.* **180–181** (2004) 421.

[17] P. Patsalas, C. Charitidis, S. Logothetidis, C. A. Dimitriadis and O. Valassiades // *J. Appl. Phys.* **86** (1999) 5296.

[18] W. D. Sproul, P. J. Rudnik and M. E. Graham // *Surf. Coat. Technol.* **39/40** (1989) 355.

[19] G. Böhm and H. Goretzki // *J. Less-Common Met.* **27** (1972) 311.

[20] F. Abele's, In: Optical Properties of Solids, ed. by F. Abele's (North-Holland, Amsterdam, 1972), p.93.

[21] S.Logothetidis, E. I. Meletis and G. Kouroulis // *J. Mater. Res.* **14** (1999) 2.